Wideband Reduced Modeling of Interconnect Circuits by Adaptive Complex-Valued Sampling Method *

Hai Wang†, Sheldon X.-D. Tan†, Gengsheng Chen‡
†Department of Electrical Engineering, University of California, Riverside, CA 92521
‡State Key Laboratory of ASIC & System, Fudan University, Shanghai, China 200433

ABSTRACT

In this paper, we propose a new wideband model order reduction method for interconnect circuits by using a novel adaptive sampling and error estimation scheme. We try to address the outstanding error control problems in the existing sampling-based reduction framework. In the new method, called *WBMOR*, we explicitly compute the exact residual errors to guide the sampling process. We show that by sampling along the imaginary axis and performing a new complex-valued reduction, the reduced model will match exactly with the original model at the sample points. We show theoretically that the proposed method can achieve the error bound over a given frequency range. Practically the new algorithm can help designers choose the best order of the reduced model for the given frequency range and error bound via adaptive sampling scheme. As a result, it can perform wideband accurate reductions of interconnect circuits for analog and RF applications. We compare several sampling schemes such as linear, logarithmic, and recently proposed re-sampling methods. Experimental results on a number of RLC circuits show that *WBMOR* is much more accurate than all the other simple sampling methods and the recently proposed re-sampling scheme with the same reduction orders. Compared with the real-valued sampling methods, the complex-valued sampling method is more accurate for the same computational costs.

1. INTRODUCTION

Model order reduction (MOR) is an efficient technique for reducing the complexity of the parasitic interconnect circuits. Existing approaches based on the Krylov subspace are very efficient [4, 13, 9, 1]. These methods perform implicit moment-matching by projecting the original system onto a Krylov subspace, are shown to preserve the stability, passivity and structure information for RLC interconnect circuits.

The Krylov subspace methods, however, suffer one long-standing problem: the lack of global error bound and designers can't predict the errors of the reduced model over a given frequency range before the reduction. Such lack of global errors is a less concern for computing wire delay, coupled noise and voltage noise of interconnects in the digital circuits where matching a few moments is sufficiently accurate, especially for RC circuits. However, for analog and RF circuits, reduced models of the extracted RLCK circuits need to be accurate for a wide frequency range and in terms of the time domain waveforms (versus delay values). The existing Krylov subspace methods can't meet such requirement although some techniques like multi-point Krylov subspace can partially mitigate this problem at high computational cost.

Other approaches based on the truncated balanced realization method (TBR) [8, 7, 10, 18] have the global error bound. But TBR methods generally suffer high computing cost and are not scalable for large circuits although some works have been made to improve the computing efficiency [19, 16, 15]. The high cost comes from computing the controllability and observability Gramians, upon which the truncation and thus reduction of weak states can be performed. This problem has been partially mitigated by the proposed Gramian approximation techniques [17, 11], where Gramians are calculated in the frequency domain by computing system impulse responses at many frequency points (samples) to approximate the Gramians. However, how to efficiently perform the sampling (how many points and which points should be chosen) to control the errors of the reduced models still remains an open problem in such sampling-based reduction methods. Recently, Silveira *et al* proposed a re-sampling scheme to resolve this issue [12]. In this approach, a statistical re-sampling scheme is used where many reduced models are computed by re-sampling from a common pool of sample points in a given frequency range. The frequencies where large variance exists among all the reduced models will be added more sample points in the next iteration. But this method may not find the best sample points to reduce the errors as it is based on the statistical information as shown in our experimental results.

In this paper, we propose to address the error control issues in the sampling-based reduction framework. The new algorithm, called *WBMOR*, consists of two important features: first, it uses the exact residual to estimate the errors of the reduced models and shows this can be done very efficiently. Second, different from existing sampling based reduction methods, *WBMOR* samples along the imaginary axis and performs new complex-valued reduction, which leads to exact matching for the reduced model at the sampled frequency points. We show theoretically that the proposed method achieves the bounded error over a given frequency range. Practically the new algorithm can help designers choose the optimal order of the reduced model for the given frequency range and error bound. It can perform wideband accurate reductions of interconnect circuits for analog and RF applications. Experimental results on a number of RLC circuits show that *WBMOR* is much more accurate than the recently proposed re-sampling scheme. Compared with the real-valued sampling methods like PMTBR [11], the complex-valued sampling method will be more accurate for the same computational costs. We also compare several sampling schemes such as linear, logarithmic sampling methods.

This paper is organized as follows: In Section 2, we review the sampling-based reduction methods. In Section 3,

*This work is supported in part by NSF grant under No. CCF-0448534, and in part by NSF grant under No. OISE-0929699. S. X.-D. Tan (stan@ee.ucr.edu) and G. Chen (gschen@fudan.edu.cn) are the corresponding authors and please contact them for potential questions regarding this paper.

978-1-4244-5766-3/10/$26.00 ©2010 IEEE

we introduce our new wideband sampling-based reduction method. Experimental results are reported in Section 4 to demonstrate the effectiveness of our proposed method. Section 5 concludes the paper.

2. REVIEW OF THE SAMPLING-BASED REDUCTION FRAMEWORK

We first consider a linear dynamic system in a standard state-space form

$$\begin{aligned} \dot{x}(t) &= Ax(t) + Bu(t) \\ y(t) &= Cx(t) \end{aligned} \tag{1}$$

where $A \in \mathbb{R}^{n\times n}$, $B \in \mathbb{R}^{n\times p}$, $C \in \mathbb{R}^{p\times n}$ and $u(t) \in \mathbb{R}^p$. Truncated balanced realization (TBR) method basically first performs the coordinate changes such that the controllability and observability (described by their corresponding Gramians) are the same for each state so that the weak states can be truncated. However, the computational cost to obtain the Gramians is $O(n^3)$ [1], which makes it too expensive for integrated circuits problems and thus an efficient Gramian approximation technique is highly appreciated.

A fast TBR method was proposed (called PMTBR) [11] to mitigate the high computational cost of standard TBR method, where the Gramians are approximated using Monte-Carlo sampling approach. Specifically, if we look at the controllability Gramian, we need to solve the following Lyapunov equation:

$$AX + XA^T + BB^T = 0 \tag{2}$$

Alternatively, the Gramian X can also be represented in frequency domain as

$$X = \int_{-\infty}^{+\infty} (j\omega I - A)^{-1} BB^T (j\omega I - A)^{-H} d\omega \tag{3}$$

where superscript H denotes Hermitian transpose. As a result, computing Gramian X boils down to evaluating the definite integral in (3) [6]. This can be done using numerical quadrature methods.

For an integral function $f(x)$, numerical quadrature methods try to approximate it as

$$\int_a^b f(x)dx \approx \sum_{k=1}^{m} w_k f(x_k) \tag{4}$$

where w_k, $k = 1, 2, ..., m$, are referred to as the quadrature point weights, while the interpolation points x_k, $k = 1, 2, ..., m$, are called quadrature points. The selections of w_k and x_k depend on the quadrature methods such as Newton-Cotes, Gaussian quadrature rules [6].

For the sampling-based reduction, our goal is not just computing the Gramian X, but the dominant eigenspace to form the projection matrix. As a result, let ω_k be the kth sample point, if we define

$$z_k = z(j\omega_k) = (j\omega_k I - A)^{-1} B \tag{5}$$

which is called kth snapshot of the system in (1) in the frequency domain. Then X can be approximated as

$$\hat{X} = \sum_{k=1}^{m} w_k z_k z_k^H = ZW^2 Z^H \tag{6}$$

where

$$Z = [z_1, z_2, \ldots, z_m] \tag{7}$$

and W is a diagonal matrix with diagonal entries $w_{kk} = \sqrt{w_k}$. w_k comes from a specific quadrature method. If we perform the singular value decomposition (SVD) on ZW and obtain

$$ZW = VSU \tag{8}$$

then V, which gives the dominant eigenspace of X, is used as the projection matrix.

3. NEW WIDEBAND SAMPLING-BASED REDUCTION METHOD

In this section, we first present how error is estimated in the proposed method. Next, we present the complex-valued reduction and some of its important properties. Last, we describe the new adaptive sampling scheme and the whole algorithm flow.

3.1 Residual based error estimation

For an interconnect circuit modeled as a RLC dynamic system with n states and p ports, the system equation (1) can be formulated as the descriptor form in the frequency domain as

$$\begin{aligned} &Gx(s) + sCx(s) = Bu(s), \\ &y(s) = Lx(s) \end{aligned} \tag{9}$$

where $G \in \mathbb{R}^{n\times n}$ and $C \in \mathbb{R}^{n\times n}$ contain elements information such as conductance, capacitance and inductance. B and L matrices describe the positions of inputs and outputs in the network respectively. And typically $B = L^T \in \mathbb{R}^{n\times p}$. $x(s) \in \mathbb{C}^n$ is the state variable vector represents node voltages and branch currents, where $s = j\omega$. Then (5) will be replaced by

$$z_k = z(s_k) = (s_k C + G)^{-1} B \tag{10}$$

After the reduction, we will have a reduced model

$$\begin{aligned} &\hat{G}x_r(s) + s\hat{C}x_r(s) = \hat{B}u(s), \\ &y_r(s) = \hat{L}x_r(s) \end{aligned} \tag{11}$$

where $\hat{G} = V^T GV$, $\hat{C} = V^T CV$, $\hat{B} = V^T B$, $\hat{L} = LV$. V is the projection matrix computed from the reduction method and $V \in \mathbb{R}^{n\times q}$. $q \ll n$ is the dimension of the reduced system. $x_r(s) \in \mathbb{C}^q$ is the reduced state vector in the reduced system.

The approximate state $\tilde{x}(s) \in \mathbb{C}^n$ is computed as

$$\tilde{x}(s) = Vx_r(s) \approx x(s) \tag{12}$$

Assume we have p impulse inputs $u(s) = \{e_1, e_2, ..., e_p\}$ applied to the system in (9), where e_i is a $p \times 1$ vector whose ith position is 1 and the rest is 0. As a result, the corresponding responses $x(s)$ will equal to $z(s) \in \mathbb{C}^{n\times p}$. Also in the reduced system, we have $x_r(s) = z_r(s) \in \mathbb{C}^{q\times p}$ defining $z_r(s) = (\hat{G} + s\hat{C})^{-1}\hat{B}$. From now on, we will use $z(s)$ and $z_r(s)$ instead of $x(s)$ and $x_r(s)$ for the identity $u(s)$ case. Plugging $\tilde{z}(s) = Vz_r(s) \approx z$ into the new state equation

$$Gz(s) + sCz(s) = B \tag{13}$$

will lead to the error matrix, which is called *residual* matrix in the paper

$$R(s) = GVz_r(s) + sCVz_r(s) - B \tag{14}$$

where $R(s) \in \mathbb{C}^{n\times p}$. Notice that if $\tilde{z}(s) = Vz_r(s)$ is very close to $z(s)$, the residual should be very small. As a result, the norm of $R(s)$, $||R(s)||$ can serve as a good error indicator for the reduced model.

We remark that $R(s)$ is not a dimensionless quantity for each element in it. Each element in it actually represents either node voltage or branch current residual. And each column of $R(s)$ can be viewed as normalized error at all the nodes/branches of the system (11) excited by the impulse response applied at one port. As a result, the residual matrix $R(s)$ can be used as the input-normalized error indicator.

3.2 New complex-valued sampling based reduction method

3.2.1 Sampling along the imaginary axis

Existing reduction techniques based on Krylov subspace method are mainly expanded at $s = 0$, while multi-point expansion methods and fast TBR methods are expanded at multiple frequency points, but along the real axis. In other words, $s = \omega$ instead of $s = j\omega$ used in (5) and (6). The reason is that if $s = j\omega$, the moments in Krylov subspace methods and snapshots in the sampling based approaches will become complex, causing the reduced matrices $\hat{G}$, $\hat{C}$, $\hat{B}$ and $\hat{L}$ to be complex matrices. This complex reduced system does not exist in the real world and is hard to be realized into a reduced RLC circuit. We notice that expanding along the imaginary axis is not an issue for explicit moment matching method like AWE and CFH methods [3] as complex Padé approximation can be carried out to compute the poles and residuals.

In this paper, we propose a new sampling scheme called Complex-Valued Sampling based Truncated Balanced Realization (*CVSTBR*) which samples along the imaginary axis $s = j\omega$ to preserve the physical meaning of the Gramian approximation. The new *CVSTBR* method can still result the **real** reduced system. We show that the resulting reduced system matches exactly with the original system at the sample points, which is not the case for sampling along the real axis (except for $s = 0$).

Algorithm 1: CVSTBR algorithm

Input: Circuit: G, C, B, L; sample points: ω_k, $k = 1, 2, ..., m$; the reduced order: q.
Output: Reduced system matrices: $\hat{G}$, $\hat{C}$, $\hat{B}$, $\hat{L}$.

1. Solve $z_k = (G + j\omega_k C)^{-1} B$ for $k = 1, 2, ..., m$.
2. Combine all the solved z_k to form Z.
3. Construct the complex Gramian subspace $Z_c = [ZZ^*]$.
4. Perform economic SVD on Z_c and obtain the left singular matrix V_c and singular value matrix S. Keep only q dominant columns of V_c.
5. Rotate V_c to the real axis through multiplying the kth column of V_c with $exp(-j\phi_k)$, where ϕ_k is the phase of the kth column in the complex plane.
6. Build the reduced model $\hat{G}$, $\hat{C}$, $\hat{B}$, $\hat{L}$ using the projection matrix V_c and V_c^T.

Specifically, by performing the sampling along the imaginary axis, Z defined in (7) is a complex matrix. Let's then define Z^*, which is the conjugate of Z, and form a new complex subspace $Z_c = [Z\ Z^*]$. Also assume W is an identity matrix, we have new versions of (6) and (8) as

$$\hat{X}_c = Z_c Z_c^H \tag{15}$$

and

$$Z_c = V_c S_c U_c \tag{16}$$

As a result, we have

$$\hat{X}_c = V_c S_c U_c U_c^H S_c V_c^H = V_c S_c^2 V_c^H \tag{17}$$

which is the eigendecomposition of the approximated Gramian $\hat{X}_c$. In contrast to the complex $\hat{X}$ in (6), $\hat{X}_c$ here is a symmetric real matrix even though Z_c is complex. According to the properties of the eigendecomposition, being the eigenspace of a symmetric real matrix, V_c should be a real unitary matrix, i.e. $V_c^H = V_c^T$, which will generate the real reduced systems even if we sample along the imaginary axis.

Note that we do not perform the eigendecomposition to compute V_c, instead, we use SVD on Z_c. However, V_c is still not a real matrix in general. The reason is that the singular vectors of the SVD are not unique in the complex plane although the singular values are uniquely computed [14]. For instance, for an SVD of matrix $\mathcal{A} \in \mathbb{C}^{n\times n}$, $\mathcal{A} = VSU^T = \sum_{i=1}^{n} \sigma_i v_i u_i^T = \sum_{i=1}^{n} \sigma_i (v_i e^{j\phi})(u_i^T e^{-j\phi})$. In other words, singular vector v_i and u_j can rotate with the same angle but in the opposite directions without changing the subspace. Specifically, for the kth column v_k in V_c, multiplying with $exp(-j\phi_k)$ will rotate it to the real axis. The phase ϕ_k is the angle between v_k and the real axis.

The new complex-valued sampling based reduction method is summarized in Algorithm 1.

3.2.2 Exact matching at sample points

In this section, we show the reduced model generated by the new sampling scheme has exact frequency responses at the sample points.

Recall that the approximated impulse response is defined as

$$\tilde{z}(j\omega) = V_c z_r(j\omega) \tag{18}$$

which can be also written as

$$\tilde{z}(j\omega) = V_c (V_c^T Q V_c)^{-1} V_c^T Q z(j\omega) \tag{19}$$

where $Q = (G + j\omega C)$ for simplicity [5].

Let's denote $P = V_c (V_c^T Q V_c)^{-1} V_c^T Q$. Since $P^2 = P$, it is clear that the matrix P is a projector along $Q^T V_c$ onto V_c. Also notice that P is a function of $j\omega$. Then, (19) can be rewritten as

$$\tilde{z}(j\omega) = P z(j\omega) \tag{20}$$

We have the following theoretical result:

THEOREM 1. *If there are m sample points $\omega_1, \omega_2, ..., \omega_m$, then $\tilde{z}(j\omega_k) = z(j\omega_k)$ for $k = 1, 2, ..., m$.*

PROOF. Assume we have m sample points $\omega_1, \omega_2, ..., \omega_m$. V_c, which is the left singular matrix from the SVD, spans the range space of Z_c:

$$span(V_c) = span(z(j\omega_1), ..., z(j\omega_m), z(j\omega_1)^*, ..., z(j\omega_m)^*) \tag{21}$$

that is, $z(j\omega_k) \in V_c$ for $k = 1, 2, ..., m$.

According to the definition of projection, P, which is a projector onto V_c, is the identity operator on the space spanned by V_c, that is, $\forall z(j\omega) \in V_c : Pz(j\omega) = z(j\omega)$. Thus, from (20),

$$\tilde{z}(j\omega_k) = z(j\omega_k),\ k = 1, 2, ..., m$$

□

Then we revisit the residue of the system defined as

$$R(j\omega) = G\tilde{z}(j\omega) + j\omega C\tilde{z}(j\omega) - B \tag{22}$$

From Theorem 1, it is easy to see that at the sample points, we have $R(j\omega_k) = 0$, where $k = 1, 2, ..., m$.

This result leads to:

COROLLARY 1. *The reduced system has zero residue at the sample points.*

Now, consider the reduced transfer function $\hat{H}(j\omega)$. At the sample points, there is $\tilde{z}(j\omega_k) = z(j\omega_k)$, thus

$$\hat{H}(j\omega_k) = L\tilde{z}(j\omega_k) = Lz(j\omega_k) = H(j\omega_k)$$

where $k = 1, 2, ..., m$. We have the following result:

COROLLARY 2. *The reduced system has the exact frequency response at the sample points.*

3.3 Adaptive sample point placement

Now we show how to place the sample points along the imaginary axis in an adaptive way.

Before we present the new method, we show some theoretical results regarding to the residual errors and the complex-valued sampling.

THEOREM 2. *Given sufficient sample points in imaginary axis, the residual function defined in* (22) *will become monotone decreasing.*

PROOF. Based on the Corollary 2, we know that at the sample points, the responses of the reduced model match exactly with those of the original model. Their residuals are all zero. The sampling approach can be viewed as the multi-point complex Krylov subspace method where only the zero-th moment is matched at every frequency point. For any frequency point $j\omega_k$, the reduced state response in (11) can be written in the moment form as

$$z_r(j\omega_k + \sigma) = (I + \sigma M_k + \sigma^2 M_k^2 + ...)\mathbf{r}_k \qquad (23)$$

where $M_k = -(\hat{G} + j\omega_k\hat{C})^{-1}\hat{C}$ and $\mathbf{r}_k = (\hat{G} + j\omega_k\hat{C})^{-1}\hat{B}$, $\sigma \in \mathbb{C}$ is a small complex value change from $j\omega_k$.

If we sample sufficiently, σ, which can be viewed as the half distance between two adjacent points, will be small enough. As a result, the error between $z_r(j\omega_k)$ and $z_r(j\omega_k + \sigma)$ can be approximated as $\sigma M_k\mathbf{r}_k$. So the error will go down monotonically with σ when σ is small enough.

Now we look at the residual $R(j\omega_k + \sigma)$. Notice that we have $R(j\omega_k) = 0$ accord to Corollary 1. If we ignore the second order terms, we have

$$\begin{aligned} R(j\omega_k + \sigma) &= (G + (j\omega_k + \sigma)C)Vz_r(j\omega_k + \sigma) - B \\ &= R(j\omega_k) + \sigma(GVM_k + j\omega_kCVM_k + CV)\mathbf{r}_k \\ &= \sigma(GVM_k + j\omega_kCVM_k + CV)\mathbf{r}_k \qquad (24) \end{aligned}$$

As a result, the residual $R(j\omega_k + \sigma)$ will decrease monotonically with σ when σ is small enough. □

Theorem 2 basically says that if a point is getting close enough to a sampled point, its residual error becomes controllable. As a result, we know that the proposed method can always achieve the error bound by sufficient samplings. But practically, it is not necessary to sample densely over the frequency range. Instead, we develop a new adaptive sampling algorithm in which sample points are added to places with more poles near the imaginary axis and having good chances to show large residuals.

The new algorithm is demonstrated in Fig. 1 as two iterative steps. At step (a), *WBMOR* first builds a reduced model using minimum sample points which are picked in the previous iterations. Then it tests all the candidate points which are initially evenly distributed in the frequency range (in log scale). Residues are computed at all the candidate points. At step (b), *WBMOR* drops all the satisfied candidate points whose residues are smaller than the threshold from the candidate set. And for each unsatisfied point, two of its adjacent middle points are added to the candidate set. At the same time, *WBMOR* takes the *peak points*, which are the unsatisfied candidate points and are local maximums in residual values, as the sample points. The peak points are dropped from the candidate set as they have guaranteed zero residues in the next iteration. The whole process continues until there are no unsatisfied candidates left.

Although the candidate adding process in step (b) can be enabled to avoid missing the potential sample point, we notice that if the initial candidates are placed dense enough (around 100 points per decade is fairly enough in our experiments), *WBMOR* will still reach good results with cheap computational cost through only dropping the satisfied candidates without recruiting new ones.

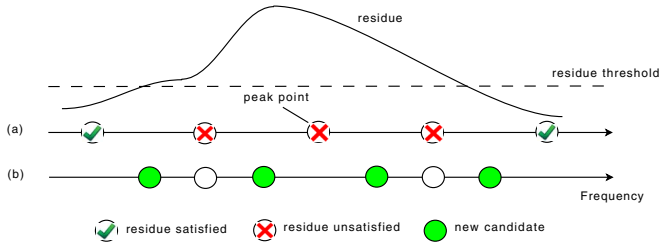

Figure 1: An illustrative example for the *WBMOR* adaptive sampling scheme.

In order to achieve a more efficient reduction, after the complex SVD on Z_c in (16), we select the dominant singular values and corresponding singular vectors in V_c based on a user set SVD threshold th_{svd}. th_{svd} is defined as the threshold for the weight of the trivial singular values.

The whole *WBMOR* flow is shown in Algorithm 2.

Algorithm 2: WBMOR algorithm

Input: Circuit: G, C, B, L; frequency range: ω_{min}, ω_{max}; the residue threshold: th_{res} and the SVD threshold: th_{svd}.
Output: Reduced system matrices: $\hat{G}$, $\hat{C}$, $\hat{B}$, $\hat{L}$.

1. Place initial candidate points at a reasonable density in the given frequency range $[\omega_{min}, \omega_{max}]$ evenly in log scale.
2. Obtain the initial reduced model by sampling at ω_{min} and ω_{max} using the *CVSTBR* algorithm.
3. While max residue $> th_{res}$, do
4. Calculate the residues at the candidate points using (22).
5. Scan all the candidate points. If residue $< th_{res}$, drop this point; otherwise (optional), add two middle points between the current point and two adjacent points as new candidate points.
6. Add the candidates which are peak points with excessive residues as the sample points. Use the *CVSTBR* algorithm to compute the new reduced model with all the selected sample points.
7. Take the singular subspace V_c from the *CVSTBR* in the last iteration. Only keep its dominant singular vectors according to th_{svd}.
8. Build the real reduced model $\hat{G}$, $\hat{C}$, $\hat{B}$, $\hat{L}$ using the projection matrix V_c and V_c^T.

4. EXPERIMENTAL RESULTS

The implementation and settings for the *WBMOR* and re-sampling method are presented as follows. For our *WBMOR* method, the residue threshold is chosen to be 0.1 and the number of initial points per decade is 100 and we only drop candidate points without adding new points. The SVD threshold th_{svd} is 10^{-7}. For the re-sampling method, the number of points in the pool is 20, the number of reduced models used in each iteration is 10, the size of the reduced model is 20. We also used 20 search points, 1/3 of which will be replaced. One point in the pool will be substituted in every iteration. We also implemented the speedup techniques such as efficient construction of projectors and heuristic search [12].

We first show the results of the static complex-valued sampling based reduction method using the transmission line (TL) model [2]. Then, we show the results of the adaptive *WBMOR* method on TL and PEEC models [2]. Finally, the runtime and maximum error of each method are evaluated using more RLC circuits.

1	2	3	4	5	6	7	8	9	10	11	12
Ckt	Node	Port	Order	WBMOR		Re-sampling		Linear		Logarithmic	
				Time(s)	Max error	Time(s)	Max error	Time(s)	Max error	Time(s)	Max error
TL	256	2	37	0.9	0.3	1.4	21.6	0.09	9.5	0.09	17.7
PEEC	480	1	79	1.9	1.5	2.4	2000.1	0.72	57.3	0.70	32.9
rlc1	640	1	62	0.7	0.1	1.2	1.1	0.13	3.4	0.12	2.08
rlc2	1180	2	160	4.8	0.1	4.4	0.5	0.37	0.6	0.34	1.6
rlc3	2680	3	192	12.1	0.1	8.8	1.2	0.9	1.3	0.8	1.5
rlc4	10960	1	58	11.2	0.2	6.3	1.0	2.7	3.6	2.7	2.1

Table 1: Scalability comparison of runtime and relative errors for *WBMOR* and the re-sampling method.

4.1 Comparison of complex-valued sampling scheme and real-valued sampling scheme

First, we would like to show the accuracy of *CVSTBR*. Note that in order to generate the same dimension of Z_c, the real sampling method has to use two times more sample points. In the example, the real sampling method uses 100 sample points that are uniformly distributed in the given frequency range while the *CVSTBR* picks only half of these points, that is 50 points. After SVD, both of the two methods keep 50 dominant columns of the left singular matrix V_c as the projection matrix, and thus the size of the two final reduced models is 50. All the samplings are generated randomly so that the real-valued sampling method is similar to the proposed PMTBR method [11]. Fig. 2 shows the results

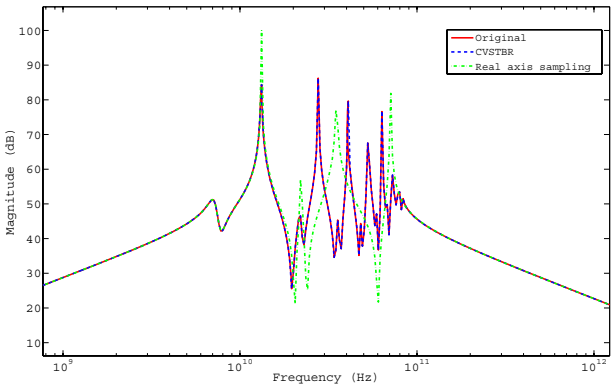

Figure 2: Accuracy comparison of imaginary axis sampling and real axis sampling methods.

of the comparison. It is clear that the model generated by the *CVSTBR* reaches a frequency response that cannot be distinguished from the original one while the real sampling method has very large errors.

For the computational cost, since both schemes generate the same dimension of the Z_c matrix, they have the same SVD cost of Z_c. However, the real axis sampling scheme samples twice more than the *CVSTBR* to reach the same size of Z_c, and thus, it is *more expensive*. To make the computational cost similar, the real axis sampling method will sample half of the points (both method sample 50 points). Obviously, it will become further inaccurate. As a result, we can clearly observe that *given the same computing cost*, the complex-valued method *CVSTBR* is more accurate than the real axis sampling method like PMTBR [11]. Actually, this is the case for all the other benchmarks we tested for the reasonable number of samples.

Detailed analysis shows that instead of 50 sample points, only 13 points are enough to produce the 50 states reduced model in the ideal case (recall that every point generates 4 states in the final reduced model without the SVD process). This ideal case happens when we sample at only the critical points such that in the SVD process, all the singular vectors are important and cannot be truncated. In the next section, we will show how we can concentrate our samplings in those critical regions in the *WBMOR* algorithm.

4.2 Adaptive process and accuracy comparison

We now compare the new adaptive *WBMOR* method with several methods based on real axis sampling, including the recently proposed re-sampling method [12], the simple linear and logarithmic sampling methods. In order to reach a fair comparison, we set all of the four methods with the same dimension of Z_c and the same size of final reduced system after SVD.

The first example we show is the transmission line model used in 4.1. In this case, *WBMOR* uses only 14 sample points and generates a reduced model of dimension 37. Fig. 3 shows the residue convergence process of our *WBMOR* during four iterations. The max residue of the reduced system drops very fast from the value as large as 10^4 to below 10^{-3} after four iterations. From Fig. 4, it is clear that our

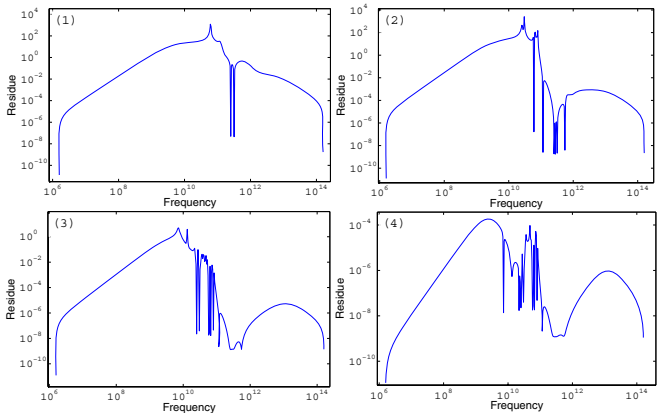

Figure 3: The residue convergence process of *WBMOR* for four iterations.

WBMOR method produced a reduced model as accurate as the the static *CVSTBR* (Fig. 2) with much less sample points and more compact size. Even with twice number of samples, the performances of all the real axis sampling based methods are disappointing, including the adaptive re-sampling method.

Fig. 5 shows the results of the widely used PEEC model. With 42 sampling points, *WBMOR* shows good results in most of the frequency bands and only a little off around $10Hz$. This is because the frequency responses at these frequencies are quite small (around -160dB) and are very hard to match due to the numerical errors.

4.3 CPU runtime and error comparison

Finally, we report the runtime and the maximum relative errors of the examples in 4.2 together with several additional RLC circuits in Table 1. The errors are relative and are com-

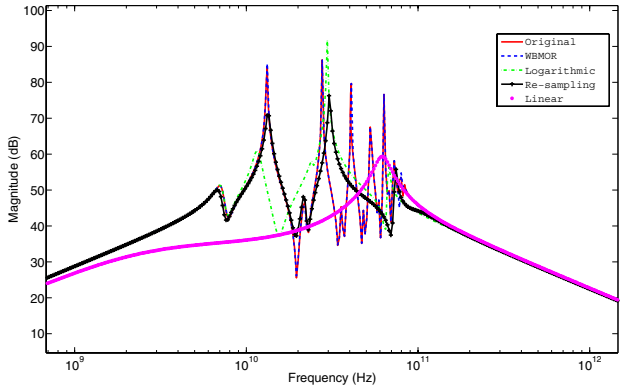

Figure 4: Comparison with re-sampling method on the transmission line example.

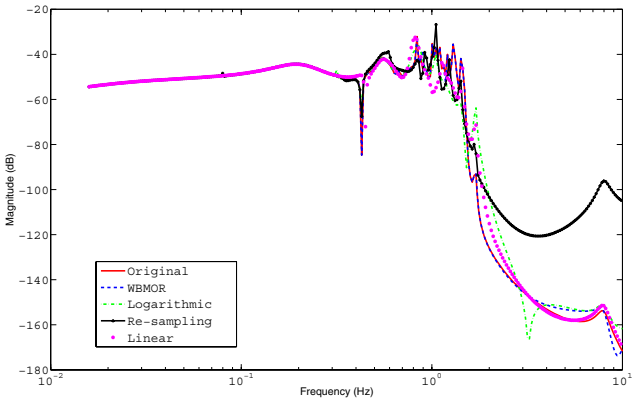

Figure 5: Comparison with re-sampling method on the PEEC example.

puted as $error(j\omega) = \frac{||H(j\omega)-\hat{H}(j\omega)||}{||H(j\omega)||}$ at all the simulation frequency points.

We observe that the proposed method is much more accurate than all the other methods, which shows the proposed method works quite well. Compared with the similar adaptive re-sampling method, the proposed method's relative errors can be order of magnitude smaller than the re-sampling method, while it takes about 2X CPU time in the largest case. It is a quite good trade-off in general.

5. CONCLUSION

We have proposed a novel wideband frequency model order reduction method *WBMOR* for interconnect circuits. We explicitly compute the exact residual errors to guide the sampling process. We show that by sampling along the imaginary axis and performing a new complex-valued sampling based reduction, the reduced model will match exactly with the original model at the sample points. Theoretically we show that the proposed method can achieve the error bound over a given frequency range with sufficient sampling. Practically we design an adaptive scheme to help designers choose the best order of the reduced model for the given frequency range and error bound. We compare several sampling schemes such as linear, logarithmic, and recently proposed re-sampling methods. Experimental results on a number of RLC circuits have shown that *WBMOR* is much more accurate than all the other simple sampling methods and the recently proposed re-sampling scheme with the same reduction orders. Compared with the real-valued sampling methods, the complex-valued sampling method is more accurate for the same computational costs.

6. REFERENCES

[1] A. C. Antoulas, *Approximation of Large-Scale Dynamical Systems*. The Society for Industrial and Applied Mathematics (SIAM), 2005.

[2] Y. Chahlaoui and P. V. Dooren, "A collection of benchmark examples for model reduction of linear time invariant dynamical systems," SLICOT Working Note 2002-2, February 2002.

[3] E. Chiprout and M. S. Nakhla, "Analysis of interconnect networks using complex frequency hopping," *IEEE Trans. on Computer-Aided Design of Integrated Circuits and Systems*, vol. 14, no. 2, pp. 186–200, Feb. 1995.

[4] P. Feldmann and R. W. Freund, "Efficient linear circuit analysis by Pade approximation via the Lanczos process," *IEEE Trans. on Computer-Aided Design of Integrated Circuits and Systems*, vol. 14, no. 5, pp. 639–649, May 1995.

[5] A. Galántai, *Projectors and Projection Methods*. Kluwer Academic Publishers, 2004.

[6] A. Iserles, *A First Course in the Numerical Analysis of Differential Equations*, 3rd ed. Cambridge University, 1996.

[7] M. Kamon, F. Wang, and J. White, "Generating nearly optimally compact models from Krylov-subspace based reduced-order models," *IEEE Trans. on Computer-Aided Design of Integrated Circuits and Systems*, vol. 47, no. 4, pp. 239–248, 2000.

[8] B. Moore, "Principal component analysis in linear systems: Controllability, and observability, and model reduction," *IEEE Trans. Automat. Contr.*, vol. 26, no. 1, pp. 17–32, 1981.

[9] A. Odabasioglu, M. Celik, and L. Pileggi, "PRIMA: Passive reduced-order interconnect macromodeling algorithm," *IEEE Trans. on Computer-Aided Design of Integrated Circuits and Systems*, pp. 645–654, 1998.

[10] J. R. Phillips, L. Daniel, and L. M. Silveira, "Guaranteed passive balancing transformation for model order reduction," *IEEE Trans. on Computer-Aided Design of Integrated Circuits and Systems*, vol. 22, no. 8, pp. 1027–1041, 2003.

[11] J. R. Phillips and L. M. Silveira, "Poor man's TBR: a simple model reduction scheme," *IEEE Trans. on Computer-Aided Design of Integrated Circuits and Systems*, vol. 24, no. 1, pp. 43– 55, 2005.

[12] L. M. Silveira and J. R. Phillips, "Resampling plans for sample point selection in multipoint model-order reduction," *IEEE Trans. on Computer-Aided Design of Integrated Circuits and Systems*, vol. 25, no. 12, pp. 2775–2783, 2006.

[13] M. Silveira, M. Kamon, I. Elfadel, and J. White, "A coordinate-transformed Arnoldi algorithm for generating guaranteed stable reduced-order models of RLC circuits," in *Proc. Int. Conf. on Computer Aided Design (ICCAD)*, 1996, pp. 288–294.

[14] L. N. Trefethen and D. Bau, III, *Numerical Linear Algebra*. The Society for Industrial and Applied Mathematics (SIAM), 1997.

[15] D. Vasilyev and J. White, "A more reliable reduction algorithm for behavioral model extraction," in *Proc. Int. Conf. on Computer Aided Design (ICCAD)*, 2005, pp. 813–820.

[16] N. Wang and V. Balakrishnan, "Fast balanced stochastic truncation via a quadratic extension of the alternating direction implicit iteration," in *Proc. Int. Conf. on Computer Aided Design (ICCAD)*, 2005, pp. 801–805.

[17] K. Willcox and J. Peraire, "Balanced model reduction via the proper orthogonal decomposition," *AIAA Journal*, 2002.

[18] B. Yan, S. X.-D. Tan, P. Liu, and B. McGaughy, "SBPOR: second-order balanced truncation for passive model order reduction of RLC circuits," in *Proc. Design Automation Conf. (DAC)*, 2007, pp. 158–161.

[19] Y. Zhou, *Numerical methods for large scale matrix equations with applications in LTI system model reduction (Ph.D. Thesis)*. Rice University, 2002.